Article

2,4,5-Trimethylimidazolium Scaffold for Anion Recognition Receptors Acting Through Charge-Assisted Aliphatic and Aromatic C–H Interactions.

Paula Sabater, Fabiola Zapata, Antonio Caballero, Israel Fernandez, Carmen Ramirez de Arellano, and Pedro Molina

Just Accepted

2,4,5-Trimethylimidazolium Scaffold for Anion Recognition Receptors Acting Through Charge-Assisted Aliphatic and Aromatic C–H Interactions.

Paula Sabater, [†] Fabiola Zapata,[†] Antonio Caballero,* [†] Israel Fernández,[‡] Carmen Ramirez de Arellano, [#] Pedro Molina*[†]

[†] Departamento de Química Orgánica, Universidad de Murcia, Campus de Espinardo, 30100, Murcia, Spain.

[‡] Departamento de Química Orgánica I, Facultad de Ciencias Químicas, Universidad Complutense, E-28040 Madrid, Spain.

[#] Departamento de Química Orgánica, Universidad de Valencia, E-46100 Valencia, Spain

ABSTRACT: A series of two-armed 2,4,5-trimethylimidazolium-based oxoanion receptors, which incorporate two end-capped photoactive anthracene rings, being the central core an aromatic or heteroaromatic ring, has been designed. In the presence of $HP_2O_7^{3-}$, $H_2PO_4^-$ and SO_4^{2-} anions, ^1H- and ^{31}P-NMR spectroscopical data clearly indicate the simultaneous occurrence of several charge-assisted aliphatic and aromatic C-H noncovalent interactions: i.e. significant downfield shifts were observed for the imidazolium $C(2)$-CH_3 protons, the methylene N-CH_2 protons and the inner aromatic proton, or the outer heteroaromatic protons. Density Functional Theory calculations confirm the occurrence of these noncovalent interaction and suggest that the interaction between the anions and the receptors is mainly electrostatic in nature.

INTRODUCTION

Given the importance of anions in the natural world, it is not surprising that considerable effort within the area of supramolecular chemistry has been devoted to the design and synthesis of receptors able to recognize selectively anionic species. In this context, a wide variety of NH donor groups have been used for hydrogen bonding-based anion recognition receptors.[1] Recently, the supramolecular arsenal has been reinforced by new items, namely receptors based either on neutral or cationic CH hydrogen bond donors groups,[2] halogen bonding (XB), which refers to a noncovalent interaction operating between an electrophilic region developed of a halogen atom and Lewis bases,[3] and anion-π interactions, an tractive force between an electron-deficient π aromatic moiety and an

anion.[4] The synthesis of selective anion receptors based on these types of interactions represents a significant advance in the field of supramolecular chemistry.

The venerable imidazole ring has played a multifaceted key role in the rational design of structural motifs for anion recognition. This simple ring system acts as an excellent hydrogen bond donor unit in synthetic anion receptor systems. In addition, the acidity of the NH proton can be tuned by changing the electronic nature of the imidazole substituents.[5] Moreover, imidazolium cations provide both a charge and relatively C(2)-H hydrogen bond donor groups to bind anionic species,[6] whereas 2-haloimidazolium-based receptors have been used for obtaining charged bipodal, imidazoliophane systems, interlocked rotaxane anion receptors, and sensing systems.[7] Recently, Beer and co-workers have explored the 2-methylimidazolium and 4,5-dimethylimidazolium derivatives in anion templated pseudorotaxanes and rotaxanes. However, despite the solid state evidences, no interactions between the different methyl protons of the imidazolium ring with anions were detected in solution phase.[8]

In this context, considering the great versatility showed by the imidazole ring to act as anion receptor under different decoration patterns (Figure 1), and also the relatively few examples reported on interactions between anions and aliphatic CH hydrogen-bond donors,[9] we wish to report a series of two-armed 2,4,5-trimethylimidazolium-based anion which provide a suitable geometric arrangement that allows four converging C(sp^3)-H and one C(sp^2)-H moieties to support oxoanion binding.
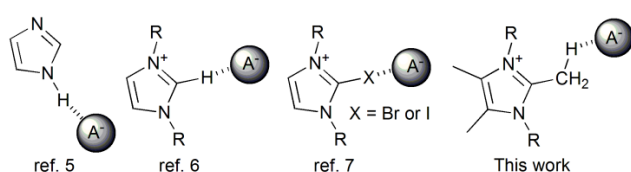
Figure 1. Different decorated imidazole rings as anion recognition binding site.

RESULTS AND DISCUSSION

Synthetic Strategy. Preparation of the target receptors **10^{2+}·2PF$_6^-$** to **13^{2+}·2PF$_6^-$** was achieved starting from 2,4,5-trimethyl-1*H*-imidazole **1**, which was obtained in grams scale following an improved procedure.[10] Subsequent alkylation with 1,3-bis(bromomethyl)benzene **2**, 2,7-bis(bromomethyl)naphthalene **3**, 1,4-bis(bromomethyl)benzene **4** or 2,6-bis(bromomethyl)pyridine **5** afforded the bis(imidazole) compounds **6-9** respectively, which by reaction with 9-(bromomethyl)anthracene provided the desired bis-imidazolium receptors as bromide salts in moderate to good yields (22-61%). Further counteranion exchange upon addition of aqueous NH$_4$PF$_6$ produced the desired **10^{2+}·2PF$_6^-$** to **13^{2+}·2PF$_6^-$** receptors (Scheme 1).

Scheme 1. Synthesis of the bis-imidazolium receptors $10^{2+} \cdot 2PF_6^-$-$13^{2+} \cdot 2PF_6^-$. Reagents and conditions: a) NaOH in H_2O and 1,3-bis(bromomethyl)benzene 2, 2,7-bis(bromomethyl)naphthalene 3, 1,4-bis(bromomethyl)benzene 4 or 2,6-bis(bromomethyl)pyridine 5 in acetonitrile; b) 9-(bromomethyl)anthracene (22-61%); c) wash with saturated NH_4PF_6 (aq).
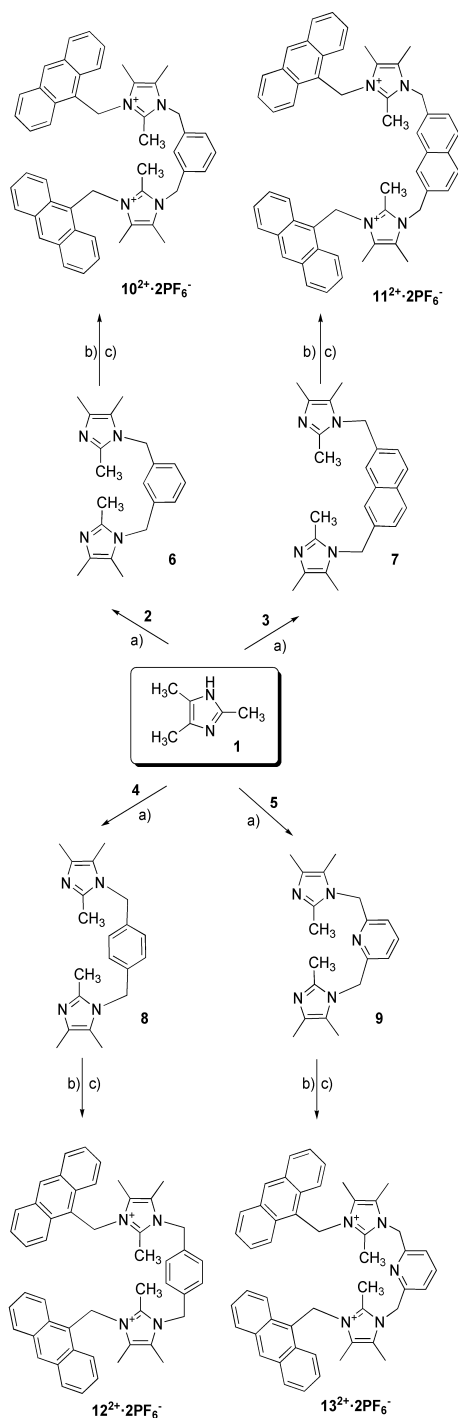
The structure of compound $13^{2+} \cdot 2PF_6^- \cdot (CH_3CN)$ was determined by single crystal X-ray diffraction (Figure 2). In the structure, the receptor is folded showing a dihedral angle between both anthryl groups of 88.68(6)° and both triazolyl groups being almost parallel to every second anthryl group (dihedral angles of 9.08(9)° and 10.62(12). The receptor is connected to the $[PF_6]^-$ anions through C-H··F hydrogen bonds with the pyridine, methyl and methylene groups acting as hydrogen bond donors. The stronger

interactions found are C(3)-H(3)···F(11) [H(3)···F(11) 2.54 Å, C(3)···F(11) 3.374(4) Å, C(3)-H(3)···F(11) 146.3°], C(20)-H(20A)···F(16)^i [i: -x+3/2, y+1/2, -z+1/2, H(20A)···F(16)^i 2.47 Å, C(20)···F(16)^i 3.351(5) Å, C(20)-H(20A)···F(16)^i 148.5°], C(20)-H(20B)···F(4)^{ii} [ii: x, y+1, z, H(20B)···F(4)^{ii} 2.56 Å, C(20)···F(4)^{ii} 3.439(4) Å, C(20)-H(20B)···F(4)^{ii} 147.5°], C(26)-H(26B)···F(4)^{ii} [H(26B)···F(4)^{ii} 2.50 Å, C(26)···F(4)^{ii} 3.472(4) Å, C(26)-H(26B)···F(4)^{ii} 171.6°] and C(27)-H(27C)···F(3)^{iii} [iii: x-1, y+1, z, H(27C)···F(3)^{iii} 2.61 Å, C(27)···F(3)^{iii} 3.544(4) Å, C(27)-H(27C)···F(3)^{iii} 158.5°]. The receptor interacts with the acetonitrile solvent trhough a the methyl group forming a C-H···N hydrogen bond [C(16)-H(16B)···N(51)^{iv}, iv: -x+1/2, y-1/2, H(16B)···N(51)^{iv} 2.52 Å, C(16)···N(51)^{iv} 3.286(5) Å, C(16)-H(16B)···N(51)^{iv} 135.2°].
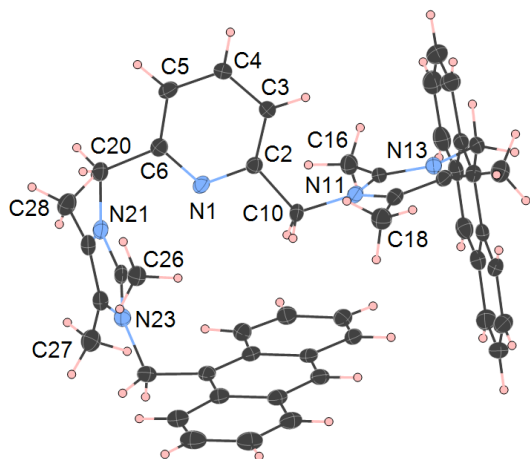

Figure 2. Ellipsoid plot (50% probability level) for the receptor **13**$^{2+}$, with the labeling scheme.

Anion Binding Studies. The anion binding properties of the receptors **10**$^{2+}$·**2PF**$_6^-$ to **13**$^{2+}$·**2PF**$_6^-$ were investigated initially by ^{1}H NMR titration experiments with the following set of anions as tetrabutylammonium salts: $HP_2O_7^{3-}$, $H_2PO_4^-$, SO_4^{2-}, HSO_4^-, NO_3^-, F^-, Cl^-, Br^-, I^-, AcO^-, ClO_4^- and $C_6H_5CO_2^-$ in CD_3CN, but a precipitate was observed during the titration of some anion, this issue was solved by utilization of the solvent mixture CD_3CN/CD_3OD (95:5 v/v).

The ^{1}H NMR spectra of receptors **10**$^{2+}$·**2PF**$_6^-$ to **13**$^{2+}$·**2PF**$_6^-$ in CD_3CN/CD_3OD (95:5 v/v) display the following characteristic signals: protons of the methyl group at C-2 (H_m), C-4 (H_k) and C-5(H_l) position of the imidazolium ring appear as a clear and sharp singlet around δ = 1.90, 2.10, and 2.05 ppm, respectively, with the exception of receptor **10**$^{2+}$·**2PF**$_6^-$ where the methyl groups at C-4 (H_k) and C-5(H_l) appear as two overlapped signals in the form of a broad singlet at δ = 2.04 ppm. Additionally, the methylene protons of the two arms N$^+$-CH$_2$-anthracene (H_j) and the N-CH$_2$-aryl (H_i) appear as two different singlets around δ = 5.20 ppm and δ = 6.25 ppm, respectively. Finally, the aromatic C–H proton (H_h) of the phenyl or naphthyl rings appears as a sharp singlet around δ = 7.00 ppm. The rest of the protons attached to the different aryl fragments (H_{f-g} and H_{a-e}) appear within the typical aromatic region at the δ = 6.77–8.73 ppm range.

Stepwise addition of the above-mentioned set of anions to a solution of the receptors $10^{2+}\cdot2PF_6^-$ to $13^{2+}\cdot2PF_6^-$ (c = 5 x 10^{-3} M) in CD$_3$CN/CD$_3$OD (95:5 v/v) showed that the selectivity of the receptors towards the set of anions tested did depend on the spacer used. Thus, the receptors $10^{2+}\cdot2PF_6^-$ and $11^{2+}\cdot2PF_6^-$ bearing a *meta*-substituted phenyl ring and 2,7-substituted naphthyl moiety, respectively, showed that the addition of HP$_2$O$_7^{3-}$, H$_2$PO$_4^-$ and SO$_4^{2-}$ anions induced significant perturbations in their corresponding ^{1}H NMR spectra. At variance, the ^{1}H NMR spectra of the receptors $12^{2+}\cdot2PF_6^-$ and $13^{2+}\cdot2PF_6^-$, bearing a *para*-substituted phenyl ring and 2,6-substituted pyridyl moiety, respectively, were only perturbed with the addition of HP$_2$O$_7^{3-}$ and SO$_4^{2-}$ anions.

The presence of the recognized anions caused similar perturbations in the ^{1}H NMR spectra of the receptors $10^{2+}\cdot2PF_6^-$ to $13^{2+}\cdot2PF_6^-$ in CD$_3$CN/CD$_3$OD (95:5 v/v). Thus, addition of increasing amounts of the anions to a solution of these receptors pro-moted a significant downfield shift in the signal corresponding to the methyl group protons (H_m) at C-2 of the imidazolium ring, ($\Delta\delta$ = 0.50-0.28 ppm for HP$_2$O$_7^{3-}$, $\Delta\delta$ = 0.39-0.28 ppm for H$_2$PO$_4^-$ and $\Delta\delta$ = 0.20-0.05 ppm for SO$_4^{2-}$). Interestingly, remarkable downfield shifts were also observed in the C(sp^3)-H methylene protons H_j (N$^+$-CH_2-anthracene, $\Delta\delta$ = 0.12-0.07 ppm) and H_j (N-CH_2-Ph, $\Delta\delta$ = 0.34-0.18 ppm). On the other hand, the signal corresponding to the methyl group (H_l) at C-4 of the imidazolium ring was considerably upfield shifted in the presence of the anions, while the signal due to the other methyl group (H_k) was also upfield shifted although in a lesser extent (Figure 3). The nature of such upfield shifts can be reasonably ascribed to an increase in the elec-tron density on the imidazolium ring upon interaction with negatively charged species.[7b]
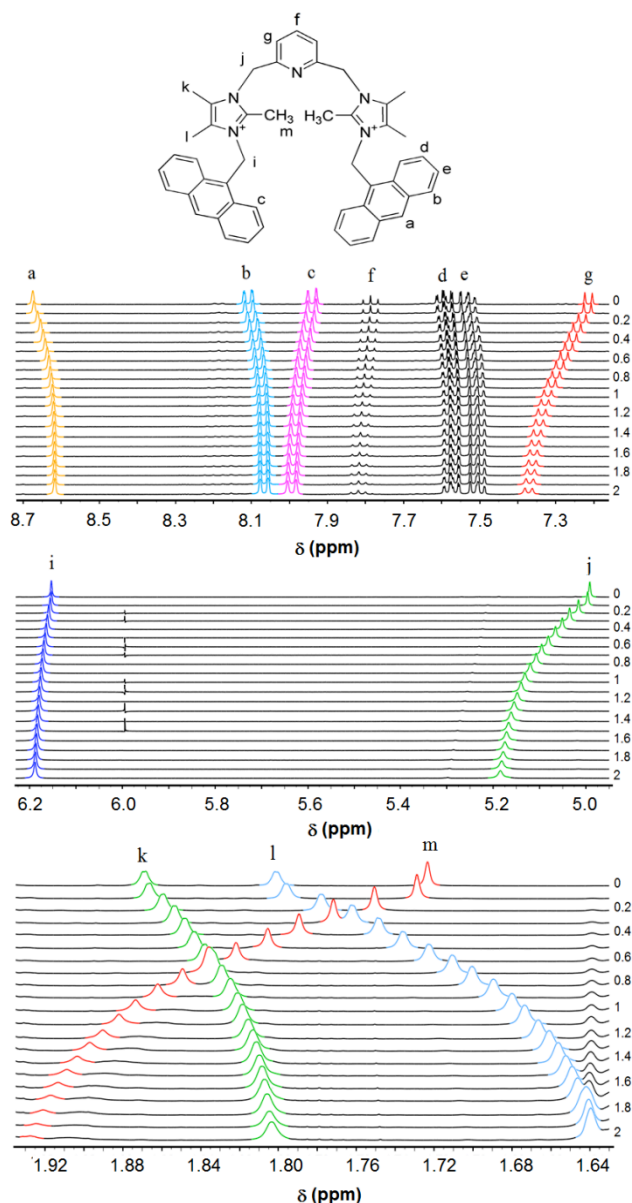
Figure 3. ^{1}H NMR spectral changes observed for the receptor $\mathbf{13^{2+} \cdot 2PF_6^-}$ (c = 5 x 10^{-3} M) in CD$_3$CN/CD$_3$OD (95:5 v/v) during the addition of HP$_2$O$_7^{3-}$ ions (up to 2 equiv).

Additionally, in the receptors $\mathbf{10^{2+} \cdot 2PF_6^-}$ and $\mathbf{11^{2+} \cdot 2PF_6^-}$, a higher downfield shift of the more acidic inner C(sp^2)-H proton (H_h) of the central core aryl ring ($\Delta\delta$ = 0.65-0.40 ppm for HP$_2$O$_7^{3-}$, $\Delta\delta$ = 0.64-0.46 ppm for H$_2$PO$_4^-$ and $\Delta\delta$ = 0.36-0.11 ppm for SO$_4^{2-}$) was observed. These changes caused in the ^{1}H NMR spectra after addition of the mentioned anions clearly suggest the occurrence of strong interactions between the anions and the receptors through neutral C(sp^2)-H and C(sp^3)-H donor groups (Figure 4).
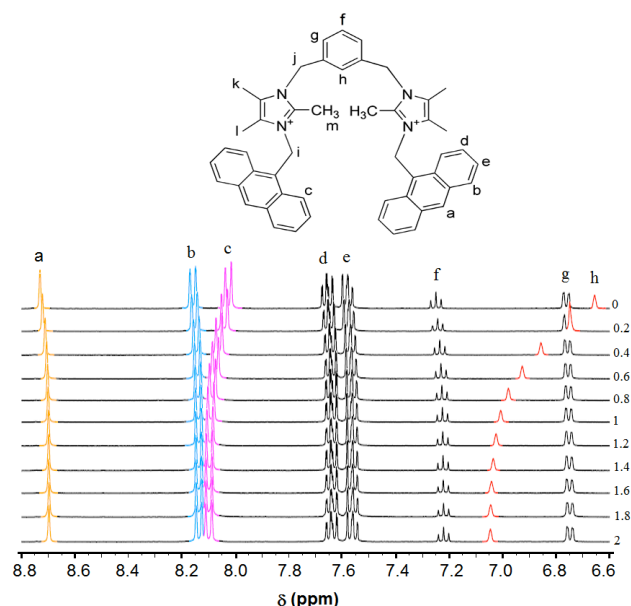
Figure 4. ^{1}H NMR spectral changes observed in the aromatic region of the receptor $\mathbf{10^{2+} \cdot 2PF_6^-}$ (c = 5 x 10^{-3} M) in CD$_3$CN/CD$_3$OD (95:5 v/v) during the addition of SO$_4{}^{2-}$ ions (up to 2 equiv).

Despite the similarities observed after the addition of these anions, a remarkable difference was detected. In the case of HP$_2$O$_7{}^{3-}$ and SO$_4{}^{2-}$ anions the maximum shift of the signals was reached after the addition of one equiv of the anions while for H$_2$PO$_4{}^-$ anions at least two equiv were required to produce a similar effect.

Job plot analysis of the titration data revealed a 1:1 anion-binding stoichiometry for HP$_2$O$_7{}^{3-}$ and SO$_4{}^{2-}$ anions and 1:2 (receptor/anion) for H$_2$PO$_4{}^-$ anions (see Supporting Information). The stoichiometry obtained for H$_2$PO$_4{}^-$ anions could be due to the ability of the monodentate H$_2$PO$_4{}^-$ anions to form stable dimers in solution in the presence of dicationic receptors.[11] The calculated association constants were obtained by fitting the titration data to the corresponding binding mode using the WinEQNMR program[12] and are gathered in Table 1.

Table 1. Association Constants for Receptors $\mathbf{10^{2+} \cdot 2PF_6^-}$ to $\mathbf{13^{2+} \cdot 2PF_6^-}$ with different anions in CD$_3$CN/CD$_3$OD (95:5 v/v) obtained from monitoring the methyl protons at C-2 of the imidazolium ring.

| Receptor	HP$_2$O$_7{}^{3-}$	H$_2$PO$_4{}^-$	SO$_4{}^{2-}$
$\mathbf{10^{2+} \cdot 2PF_6^-}$	1267 ± 130	K_{11} = 1828 ± 87	5744 ± 334
		K_{12} = 656 ± 32	
$\mathbf{11^{2+} \cdot 2PF_6^-}$	6542 ± 427	K_{11} = 4662 ± 458	3840 ± 242
		K_{12} = 258 ± 15	
$\mathbf{12^{2+} \cdot 2PF_6^-}$	2234 ± 147	—[a]	868 ± 6

| $13^{2+} \cdot 2PF_6^-$ | 853 ± 98 | $-^{[a]}$ | 3935 ± 341 |

[a] No detectable evidence of binding observed

The analysis of the obtained association constants reveal that the bis-imidazolium receptors $10^{2+} \cdot 2PF_6^-$ and $13^{2+} \cdot 2PF_6^-$, bearing the *meta*-substituted phenyl ring and the analogous 2,6-substituted pyridyl moiety, respectively, exhibit a remarkable binding affinity for SO_4^{2-} ions: $K_a = 5744 \pm 334$ M^{-1} for receptor $10^{2+} \cdot 2PF_6^-$ and $K_a = 3935 \pm 341$ M^{-1} for receptor $13^{2+} \cdot 2PF_6^-$ which are almost five times higher than those calculated for $HP_2O_7^{3-}$ (K_a $10^{2+} \cdot 2PF_6^- = 1267 \pm 130$ M^{-1} and K_a $13^{2+} \cdot 2PF_6^- = 853 \pm 98$ M^{-1}). Interestingly the utilization of a larger spacer such as naphthalene and *p*-phenyl units in receptors $11^{2+} \cdot 2PF_6^-$ and $12^{2+} \cdot 2PF_6^-$, respectively, caused an inversion in the selectivity, where the higher association constants were observed for $HP_2O_7^{3-}$ anions instead. The key role of the aromatic C(sp^2)-*H* protons pointing into the cavity is illustrated by the fact that the receptors $10^{2+} \cdot 2PF_6^-$ and $11^{2+} \cdot 2PF_6^-$ display moderate association constants for $H_2PO_4^-$ anions whereas in receptors $12^{2+} \cdot 2PF_6^-$ and $13^{2+} \cdot 2PF_6^-$ where these protons are absent no binding for $H_2PO_4^-$ anions was detected. On the other hand and for comparison purposed only it is important to note that values of the association constant for $H_2PO_4^-$ anions with 2-iodoimidazolium (halogen bonding) derivatives[7b] in DMSO and 4,5-dimethylimidazolium (hydrogen bonding) derivative[8] in CDCl$_3$ were found to be $K_a = 1100 \pm 300$ M^{-1} and $K_a = 4301 \pm 572$ M^{-1} respectively.

^{31}P NMR spectral changes of $HP_2O_7^{3-}$ and $H_2PO_4^-$ anions were also studied in the presence of 1 and 0.5 equiv of the receptors, respectively. The addition of either 1 equiv of the receptors $10^{2+} \cdot 2PF_6^-$ to $13^{2+} \cdot 2PF_6^-$ to a solution of $HP_2O_7^{3-}$ in CD$_3$CN/CD$_3$OD (95:5 v/v) or 0.5 equiv of the receptors $10^{2+} \cdot 2PF_6^-$ to $11^{2+} \cdot 2PF_6^-$ to a solution of $H_2PO_4^-$ in CD$_3$CN/CD$_3$OD (95:5 v/v) promotes an upfield shift in the ^{31}P NMR spectra of the $HP_2O_7^{3-}$ or $H_2PO_4^-$ anion around $\Delta\delta = -1.00$ ppm and $\Delta\delta = -0.50$ ppm, respectively (Figure 5). Upfield shifts of δ about -3 ppm have been reported for hydrogenpyrophosphate trianion with other receptors.[13]
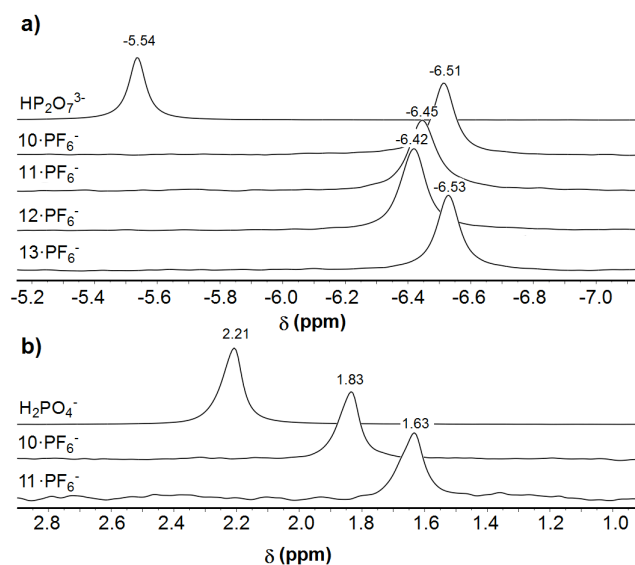
Figure 5. Changes in the ^{31}P NMR spectra of a) $HP_2O_7^{3-}$ (CD$_3$CN/CD$_3$OD 95:5) and b) $H_2PO_4^-$ in CD$_3$CN/CD$_3$OD 95:5 after the addition of different receptors.

The emission spectra of receptors $10^{2+} \cdot 2PF_6^-$ to $13^{2+} \cdot 2PF_6^-$ in CH$_3$CN (c = 2.5·10^{-6} M) when excited at λ_{exc} = 370 nm, display the typical anthracene monomeric emission bands at λ = 397, 419, 443 and 469 nm, with high quantum yields (Φ = 0.64-0.51).

The emission binding studies show that the addition of HSO_4^-, NO_3^-, Cl^-, Br^-, I^-, ClO_4^-, and BF_4^- anions does not modify significantly the intensity of the emission bands of the receptors $10^{2+} \cdot 2PF_6^-$ to $13^{2+} \cdot 2PF_6^-$ (c = 2.5 x 10^{-6} M in CH$_3$CN) while the presence of $HP_2O_7^{3-}$ (Figure 6), $H_2PO_4^-$ or SO_4^{2-} anions leads to fluorescence quenching.
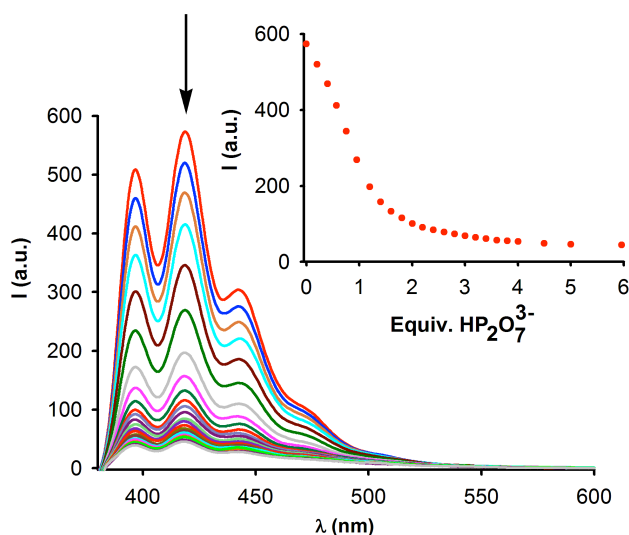

Figure 6. Changes in the fluorescence spectra of receptor $11^{2+} \cdot 2PF_6^-$ (c = 2.5 x 10^{-6} M in CH$_3$CN) upon addition of $HP_2O_7^{3-}$ anions at 20 °C. Inset: changes of emission at λ = 419 nm of receptor $11^{2+} \cdot 2PF_6^-$ upon addition of $HP_2O_7^{3-}$ anions.

The decrease of the emission bands strongly depends on the nature of the anion added. Thus, the presence of $HP_2O_7^{3-}$ anions caused the highest decrease in the fluorescent emission bands on all the receptors $10^{2+} \cdot 2PF_6^-$ to $13^{2+} \cdot 2PF_6^-$ (88-55%), followed by $H_2PO_4^-$ (51-36%) and SO_4^{2-} (39-26%) anions. Receptors $11^{2+} \cdot 2PF_6^-$ and $12^{2+} \cdot 2PF_6^-$ having the larger spacers (naphthalene and p-phenyl) showed less selectivity than the receptors $10^{2+} \cdot 2PF_6^-$ and $13^{2+} \cdot 2PF_6^-$ and also the presence of F$^-$, AcO$^-$ and PhCOO$^-$ anions caused a moderate decrease in the intensity of their emission bands (Figure 7). The decrease in the intensity of the emission bands of the receptors $10^{2+} \cdot 2PF_6^-$ to $13^{2+} \cdot 2PF_6^-$ in the presence of these anions could be attributed to a photo-induced electron transfer (PET) mechanism.[14]
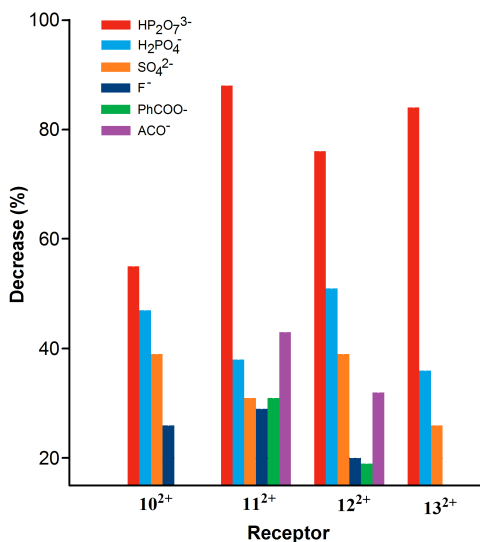
Figure 7. Graphical representation of the decrease (in percentage) in the emission intensity of the receptors $10^{2+}\cdot2PF_6^-$ to $13^{2+}\cdot2PF_6^-$ (c = 2.5 x 10^{-6} M in CH_3CN) after the addition of excess (up to 3 equivalents) of different anion.

The absorption spectra of the receptors $10^{2+}\cdot2PF_6^-$–$13^{2+}\cdot2PF_6^-$ in CH_3CN are very similar and show a strong absorption band at λ = 255 nm ($\varepsilon \sim$ 242000 $M^{-1}\cdot cm^{-1}$) along with the characteristic absorption bands attributed to the anthracene moieties at λ = 338 nm ($\varepsilon \sim$ 6000 $M^{-1}\cdot cm^{-1}$), 353 nm ($\varepsilon \sim$ 11200 $M^{-1}\cdot cm^{-1}$), 370 nm ($\varepsilon \sim$ 16100 $M^{-1}\cdot cm^{-1}$) and 390 nm ($\varepsilon \sim$ 14000 $M^{-1}\cdot cm^{-1}$). The addition of the above-mentioned set of anions to a solution of the receptors $10^{2+}\cdot2PF_6^-$–$13^{2+}\cdot2PF_6^-$ (c = 1 × 10^{-5} M) in CH_3CN demonstrates that only the addition of $H_2PO_4^-$ anions induces remarkable changes in the absorption spectra in all receptors. Thus, addition of $H_2PO_4^-$ anions promotes the decreasing of the high-energy band at λ = 255 nm while the anthracene absorption bands were red shifted by $\Delta\lambda$ = 4 nm. The presence of well defined isosbestic points at λ = 262, 364, 373, and 392 nm was also observed during the titration process (Figure 8).
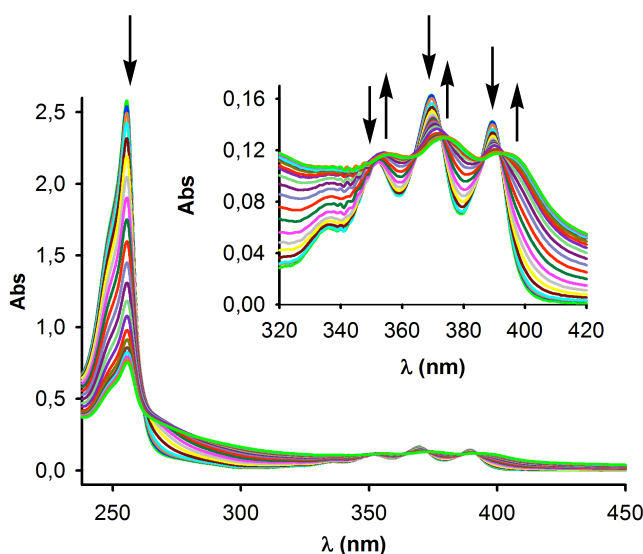
Figure 8. Changes in the absorption spectra of receptor $11^{2+} \cdot 2PF_6^-$ (c = 1 × 10^{-5} M) in CH$_3$CN upon addition of H$_2$PO$_4^-$ anions up to 4 equiv. at 20 °C. Arrows indicate the absorptions that increase or decrease during the titration.

Computational Study: Density Functional Theory (DFT) calculations were carried out to gain more insight into the nature of the interactions between receptors 10^{2+} and 13^{2+} and anions. To this end, the complexes formed upon the addition of HP$_2$O$_7^{3-}$ and SO$_4^{2-}$ anions to the model dicationic receptors $10M^{2+}$ and $13M^{2+}$, where the non-interacting anthracene groups were replaced by phenyl groups, were analyzed in detail by means of the Atoms in Molecules (AIM) and Energy Decomposition Analysis (EDA) methods.[15]

[10M-SO$_4$]

[13M-SO$_4$]
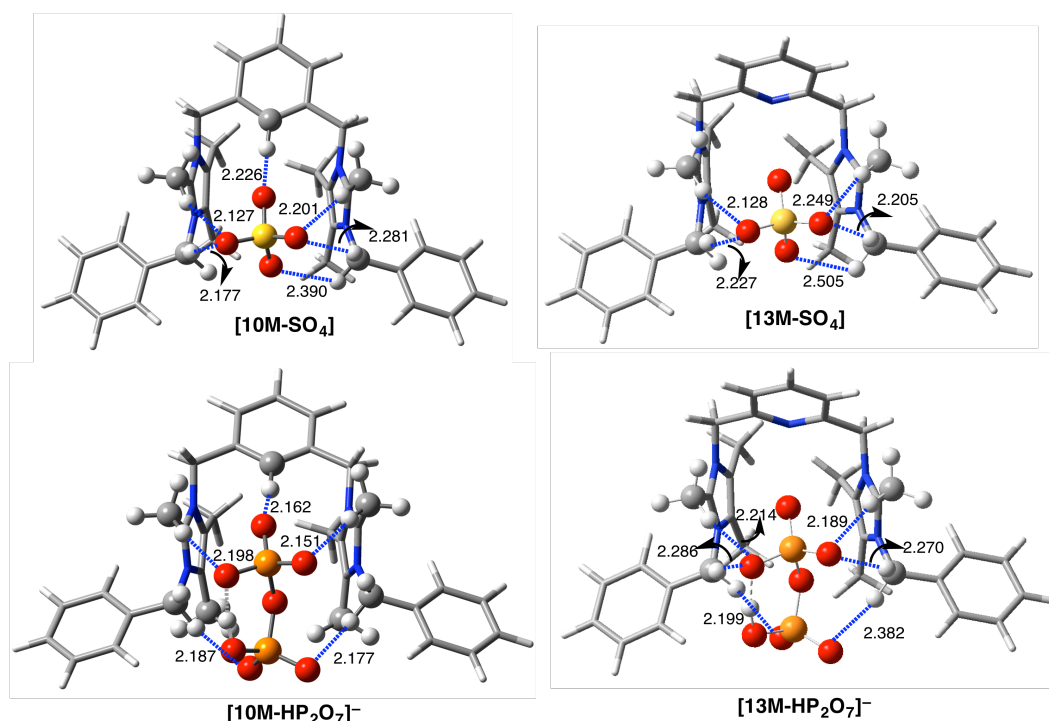
[10M-HP$_2$O$_7$]$^-$

[13M-HP$_2$O$_7$]$^-$

Figure 9. Optimized geometries of complexes **[10M-HP$_2$O$_7$]$^-$**, **[10M-SO$_4$]**, **[13M-HP$_2$O$_7$]$^-$** and **[13M-SO$_4$]**. Bond distances are given in angstroms. All data have been computed at the PCM(MeCN)-M06-2X/6-31+G(d,p) level.

The optimized geometries of complexes **[10M-HP$_2$O$_7$]$^-$**, **[10M-SO$_4$]**, **[13M-HP$_2$O$_7$]$^-$** and **[13M-SO$_4$]** (PCM(MeCN)-M06-2X/6-31+G(d,p) level, Figure 9) clearly show short contacts (i.e. shorter than the sum of the van der Waals radii, 2.72 Å)[16] between the oxygen atoms of the anions and the hydrogen atoms of the receptor (mainly, H_i, and H_m, according to the numbering in Figures 3 and 4). Moreover, complexes derived from $10M^{2+}$ present an additional interaction involving the aromatic hydrogen H_h, not possible in complexes derived from $13M^{2+}$ due to the replacement of this CH$_h$ fragment by a nitrogen atom, which is in part responsible for the higher association constants calculated for receptor 10^{2+} (see above). This CH/N replacement provokes a significant change in the equilibrium geometry of the complexes derived from $13M^{2+}$, namely the relative orientation of the pyridyl moiety with the

respect to the anion, in order to diminish the electronic repulsion between the lone-pairs of the nitrogen and oxygen atoms. Despite that, it can be concluded that both type of receptors behave similarly in terms of anion recognition.

In addition, the AIM method reveals the occurrence of bond critical points (BCPs) and bond paths (BPs) running between the oxygen atoms of $HP_2O_7^{3-}$ and SO_4^{2-} and these particular hydrogen atoms for both type of receptors (Figure 10), hence confirming the interactions established between the anions and the trimethylimidazolium scaffolds. Therefore, it can be suggested that the above described downfield shifts in the ^1H NMR titration experiments find their origin in these intermolecular $O\cdots H-C(sp^3)$ and $O\cdots H-C(sp^2)$ interactions.

Further quantitative insight into the bonding situation of the above complexes can be gained by means of the EDA-NOCV method. To this end, we focused on the interaction between **10M^{2+}** and **13M^{2+}** with the anion SO_4^{2-} in the complexes **[10M-SO$_4$]** and **[13M-SO$_4$]**, respectively. Table 2 gathers the EDA-NOCV data computed at the dispersion corrected BP86-D3/TZ2P level using the above described PCM(MeCN)-M06-2X/6-31+G(d,p) optimized geometries (Figure 9).

From the data in Table 2, it becomes clear that the interaction between the receptors **10M^{2+}** and **13M^{2+}** with SO_4^{2-} is mainly electrostatic, as viewed from the computed high ΔE_{elstat} value which contributes ca. 76% to the total attractions. This finding is not surprising if we take into account that the interacting fragments are highly charged species. Despite that, the orbital interaction is not negligible as the ΔE_{orb} term contributes ca. 18% to the total interaction energy between the cationic receptor and SO_4^{2-} fragments. Among the different orbital interactions, the EDA-NOCV method identifies the donation from the lone-pairs of the oxygen atoms of SO_4^{2-} to the vacant $\sigma^*(C-H)$ molecular orbitals of the methyl $C-H_m$, methylene $C-H_i$ and aromatic $C-H_h$ groups as the main orbital contributions to the total ΔE_{orb} term ($\Delta E = -7.6$, -8.5 and -5.9 kcal/mol, respectively, see Figure SI34 in the Supporting Information). Finally, the contribution coming from dispersion forces can be considered as negligible as the corresponding ΔE_{disp} term only amounts ca. 5% to the total bonding. In addition, our EDA-NOCV calculations also reveal that the interaction between SO_4^{2-} and the pyridyl-derived receptor **13M^{2+}** is slightly lower than that computed for **10M^{2+}** as a consequence of the lack of the aryl CH$\cdots$O interaction present in **10M^{2+}**.
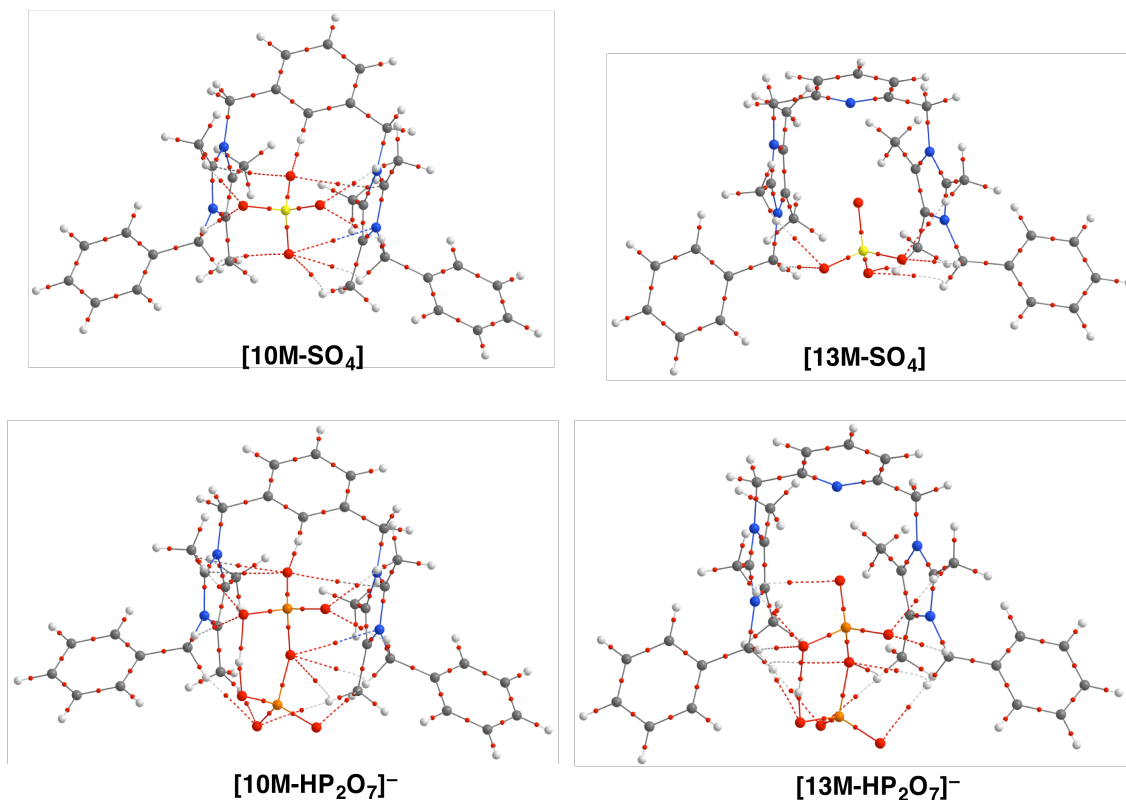
Figure 10. AIM diagrams computed for complexes [10M-HP$_2$O$_7$]$^-$, [10M-SO$_4$], [13M-HP$_2$O$_7$]$^-$ and [13M-SO$_4$]. The lines connecting the atomic nuclei are the bond paths, while the small red spheres indicate the corresponding bond critical points.

Table 2. EDA-NOCV values (in kcal/mol) for complexes [10M-SO$_4$] and [13M-SO$_4$].[a]

Complex	ΔE_{int}	ΔE_{Pauli}	ΔE_{elstat}	ΔE_{orb}	ΔE_{disp}
[10M-SO$_4$]	-330.6	52.8	-292.9	-70.2	-20.2
			(76.4%)	(18.3%)	(5.3%)
[13M-SO$_4$]	-323.7	46.8	-282.9	-67.6	-20.1
			(76.4%)	(18.2%)	(5.4%)

[a] Fragments: 11M^{2+} or 13M^{2+} and SO$_4^{2-}$ computed as close-shell singlets. The percentage values in parentheses give the contribution to the total attractive interactions, ΔE_{elstat} + ΔE_{orb} + ΔE_{disp}. All data have been computed at the BP86-D3/TZ2P//PCM(MeCN)-M06-2X/6-31+G(d,p) level.

CONCLUSION

In conclusion, the two-armed 2,4,5- trimethylimidazolium-based oxoanion receptors **10^{2+}·2PF$_6^-$** to **13^{2+}·2PF$_6^-$** have proved to be interesting benchmarks for exploring the potential of several aliphatic and aromatic C-H noncovalent interactions. The importance of these interactions is highlighted by the fact that the receptors are able to selectively interact with $HP_2O_7^{3-}$, $H_2PO_4^-$ and SO_4^{2-} anions mainly via $O\cdots H-C(sp^3)$ and $O\cdots H-C(sp^2)$ interactions. According to our DFT calculations, it can be concluded that the interaction between the anion and the receptors is mainly electrostatic in nature. Despite that, the orbital interaction is not negligible and also contributes, although in a lesser extent, to the total attraction between the receptor and the anion.

EXPERIMENTAL SECTION

General Comments. All reactions were carried out using solvents that were dried by routine procedures. All melting points were determined by means of a hot-plate melting-point apparatus and are uncorrected. Solution ^{1}H, ^{13}C, and ^{31}P NMR spectra were recorded with 200, 300, 400, or 600 MHz spectrometers. The following abbreviations have been used to state the multiplicity of the signals: s (singlet), m (multiplet), and q (quaternary carbon atom). Chemical shifts (δ) in the ^{1}H and ^{13}C NMR spectra are referenced to tetramethylsilane (TMS). Fluorescence spectra were carried out in the solvents and concentrations stated in the text and in the corresponding figure captions, using a dissolution cell with 10 mm path length, and they were recorded with the spectra background corrected before and after sequential additions of different aliquots of anions. Quantum yield values were measured with respect to anthracene as the standard ($\Phi = 0.27 \pm 0.01$) using the equation $\Phi_x/\Phi_s = (S_x/S_s)\,[(1 - 10^{-As})/(1 - 10^{-Ax})](n_s^2/n_x^2)$, where x and s indicate the unknown and standard solution, respectively, Φ is the quantum yield, S is the area under the emission curve, A is the absorbance at the excitation wavelength and n is the refractive index. Mass spectra were recorded in FAB+, mass spectra were carried out with 3-nitrobenzylalcohol as a matrix.

2,4,5-trimethyl-1H-imidazole 1. Yield 1.19 g (15 %). Acetaldehyde (3.168 g, 0.072 mol), butane-2,3-dione (6.192 g, 0.072 mol), and ammonium acetate (54.15 g, 0.7 mol) were dissolved in 90 mL of acetic acid and stirred during 24 h at room temperature. The reaction mixture was added dropwise to a solution of concentrated NH$_4$OH (300 mL) at 0 °C, diluted with 400 ml of water and extracted with AcOEt (4 x 200 mL). The organic phase was collected and the AcOEt was removed under reduced pressure to give an orange oil, which was washed with Et$_2$O to give the desired 2,4,5-trimethyl-1H-imidazole as a white solid.^{1}H NMR (400 MHz, CDCl$_3$) δ 2.32 (3H, s), 2.11 (6H, s); ^{13}C NMR (100 MHz, DMSO-d$_6$) δ 142.5, 126.7, 14.9, 11.55 ppm.; MS (ESI): *m/z* calc. for [M + H]$^+$ 111.08, found 111.08; mp = 127-129ºC; Anal. Calcd for C$_6$H$_{10}$N$_2$: C, 65.42; H, 9.15; N, 25.43. Found: C, 65.50; H, 9.27; N, 25.30.

General procedure for the synthesis of the Bis-imidazoles 6-9.

To a solution of 2,4,5-trimethyl-1*H*-imidazole (0.230 g, 2.08 mmol) in acetonitrile (15 ml) was added dropwise a solution of 1M NaOH (3.0 mmol) and stirred during 10 min. with the corresponding dibromo derivative (0.25 g, 0.95 mmol) was added in one portion and the resultant mixture was heated at reflux overnight. The solvent was removed and the resultant residue dissolved in chloroform (100 mL), which was washed with 1 M NaOH solution (50 mL) and water (2 x 25 mL). The aqueous layers were re-

extracted with 25 mL chloroform, and the combined organic layers dried over magnesium sulphate, filtered and dried *in vacuo*, giving a pure colourless oil

1,3-Bis((2,4,5-trimethylimidazol-1-yl)methyl)benzene 6. Yield 0.157 g (50%), ^{1}H NMR (400 MHz, CD$_3$CN) δ 7.29 (1H, t, *J* = 8 Hz), 6.92 (2H, d, *J* = 8 Hz), 6.45 (1H, s), 4.95 (4H, s), 2.13 (6H, s), 2.03 (6H, s), 1.92 (6H, s) ppm; ^{13}C NMR (100 MHz, CD$_3$CN) δ 143.2, 139.3, 132.0, 130.0, 125.9, 124.5, 122.6, 47.2, 13.2, 12.6, 8.9 ppm; MS (ESI): *m/z* calc. for [M + H]$^+$ 323.22, found 323.22.

2,7-Bis((2,4,5-trimethylimidazol-1-yl)methyl)naphthalene 7. Yield 0.231 g (63%), ^{1}H NMR (300 MHz, CDCl$_3$) δ 7.79 (2H, d, *J* = 9 Hz), 7.14 (2H, dd, *J* = 9 Hz, *J* = 1 Hz), 7.12 (2H, s), 5.10 (4H, s), 2.32 (6H, s), 2.19 (6H, s), 2.03 (6H, s) ppm; ^{13}C NMR (75 MHz, CDCl$_3$) δ 143.7, 135.3, 134.3, 133.1, 131.3, 129.8, 125.1, 125.0, 123.7, 48.1, 13.8, 12.9, 9.8 ppm; MS (ESI): *m/z* calc. for [M + H]$^+$ 373.23, found 373.23.

1,4-Bis((2,4,5-trimethylimidazol-1-yl)methyl)benzene 8. Yield 0.130 g (41%), ^{1}H NMR (300 MHz, CDCl$_3$) δ 6.79 (4H, s), 4.84 (4H, s), 2.16 (6H, s), 2.03 (6H, s), 1.89 (6H, s) ppm; ^{13}C NMR (75 MHz, CDCl$_3$) δ 142.5, 136.1, 131.5, 126.2, 121.8, 46.4, 13.1, 12.4, 8.8 ppm; MS (ESI): *m/z* calc. for [M + H]$^+$ 323.22, found 323.22.

2,6-Bis((2,4,5-trimethylimidazol-1-yl)methyl)pyridine 9. Yield 0.128 g (40%), ^{1}H NMR (300 MHz, CDCl$_3$) δ 7.51 (1H, t, *J* = 8 Hz), 6.51 (2H, d, *J* = 8 Hz), 5.00 (4H, s), 2.25 (6H, s), 2.11 (6H, s), 1.98 (6H, s) ppm; ^{13}C NMR (75 MHz, CDCl$_3$) δ 157.8, 143.9, 139.6, 132.8, 122.9, 119.8, 49.7, 14.3, 13.5, 9.9 ppm; MS (ESI): *m/z* calc. for [M + H]$^+$ 324.44, found 324.44.

General procedure for the synthesis of the Bis-imidazolium receptors 10^{2+}-13^{2+} as bromide salt.

To a solution of the Bis-imidazole **6-9** (0.78 mmol) in acetonitrile (25 mL) was added dropwise 40 mL a solution of 9-(bromomethyl)anthracene in acetonitrile (1.56 mmol) and the resultant mixture was heated at reflux temperature during 72 h. The volume of solvent was concentrated to 50 mL and then cooled to 0ºC. The resulting precipitate was collected and washed with diethylether, giving the desired bis-imidazolium receptor as bromide salt.

Bis-imidazolium receptor 10^{2+}·2Br$^-$. Yield 0.408 g (61%), ^{1}H NMR (400 MHz, DMSO-d$_6$) δ 8.81 (2H, s), 8.20 (4H, d, *J* = 8 Hz), 8.14 (4H, d, *J* = 8 Hz), 7.65 (4H, t, *J* = 8 Hz), 7.58 (4H, t, *J* = 8 Hz), 7.33 (1H, t, *J* = 8 Hz), 7.05 (1H, s), 6.85 (2H, d, *J* = 8 Hz), 6.48 (4H, s), 5.40 (4H, s), 2.30 (6H, s), 2.02 (6H, s), 1.77 (6H, s) ppm; ^{13}C NMR (75 MHz, DMSO-d$_6$) δ 145.2, 136.7, 132.3, 131.9, 131.3, 131.1, 131.0, 129.1, 127.9, 127.3, 127.1, 127.0, 126.6, 125.0, 124.7, 124.6, 48.8, 45.9, 12.4, 10.7, 9.7 ppm; MS (ESI): *m/z* calc. for [M^{2+}+Br$^-$]$^+$ 783.31, found 783.31; mp = 188-190 ºC; Anal. Calcd for C$_{50}$H$_{48}$Br$_2$N$_4$: C, 69.45; H, 5.59; N, 6.48. Found: C, 69.60; H, 5.50; N, 6.39.

Bis-imidazolium receptor 11^{2+}·2Br$^-$. Yield 0.135 g (22%), ^{1}H NMR (400 MHz, CD$_3$CN/ CD$_3$OD (95/5 v/v)) δ 8.58 (2H, s), 8.29 (4H, d, *J* = 8 Hz), 8.06 (4H, d, *J* = 8 Hz), 7.84 (2H, d, *J* = 8 Hz), 7.74 (2H, s), 7.62 (4H, t, *J* = 6 Hz), 7.50 (4H, t, *J* = 6 Hz), 7.30 (2H, dd, *J* = 8 Hz, *J* = 1 Hz), 6.49 (4H, s), 5.37 (4H, s), 2.24 (6H, s), 1.96 (6H, s), 1.86 (6H, s) ppm; ^{13}C NMR (100 MHz, CD$_3$CN/ CD$_3$OD (95/5 v/v)) δ 144.6, 134.5, 133.1, 133.0, 132.1, 137.1, 130.9, 130.4, 129.3, 128.6, 128.1, 126.9, 126.4, 125.5, 125.2, 124.5,

124.3, 48.9, 46.2, 12.1, 10.3, 8.9 ppm; MS (ESI): m/z calc. for $[M^{2+}+Br^-]^+$ 833.32, found 833.32; mp = 216-218 ºC; Anal. Calcd for $C_{54}H_{50}Br_2N_4$: C, 70.90; H, 5.51; N, 6.12. Found: C, 71.02; H, 5.45; N, 6.25.

Bis-imidazolium receptor $12^{2+}·2Br^-$. Yield 0.38 g (38%), ^1H NMR (400 MHz, CD$_3$CN/ CD$_3$OD (95/5 v/v)) δ 8.82 (2H, s), 8.20 (4H, d, J =8 Hz), 8.15 (4H, d, J = 8 Hz), 7.65 (4H, t, J =8 Hz), 7.56 (4H, t, J =8 Hz), 7.03 (4H,s), 6.49 (4H, s), 5.43 (4H, s), 2.34 (6H, s), 2.04 (6H, s), 1.79 (6H, s) ppm; ^{13}C NMR (100 MHz, CD$_3$CN/ CD$_3$OD (95/5 v/v)) δ 145.0, 135.6, 132.2, 131.8, 131.3, 131.0, 129.0, 128.2, 127.8, 127.2, 126.8, 124.9, 124.5, 48.5, 45.7, 12.2, 10.6, 9.6 ppm; MS (ESI): m/z calc. for $[M^{2+}+Br^-]^+$ 783.3, found 783.3; mp = 206-208 ºC; Anal. Calcd for $C_{50}H_{48}Br_2N_4$: C, 69.45; H, 5.59; N, 6.48. Found: C, 69.38; H, 5.48; N, 6.60.

Bis-imidazolium receptor $13^{2+}·2Br^-$. Yield 0.227 g (34%), ^1H NMR (400 MHz, DMSO-d$_6$) δ 8.77 (2H, s), 8.15 (4H, d, J = 8 Hz), 8.07 (4H, d, J = 8 Hz), 7.90 (1H, t, J = 8 Hz), 7.60 (4H, t, J = 7 Hz), 7.54 (4H, t, J = 7 Hz), 7.36 (2H, d, J = 8 Hz), 6.30 (4H, s), 5.32 (4H, s), 2.09 (6H, s), 1.85 (6H, s), 1.65 (6H, s) ppm; ^{13}C NMR (100 MHz, DMSO-d$_6$) δ 154.8, 145.1, 140.3, 132.1, 131.7, 131.3, 130.9, 129.0, 127.4, 127.2, 126.8, 124.6, 124.5, 123.2, 50.1, 45.5, 11.9, 10.4, 9.3 ppm; MS (ESI): m/z calc. for $[M^{2+}+Br^-]^+$ 785.83, found 785.83; mp = 194-196 ºC; Anal. Calcd for $C_{49}H_{47}Br_2N_5$: C, 67.98; H, 5.47; N, 8.09. Found: C, 67.88; H, 5.39; N, 8.05.

General procedure for the synthesis of the Bis-imidazolium receptors 10^{2+}-13^{2+} as hexafluorophosphate salt.

A solution of bis-imidazolium receptor as bromide salt **$10^{2+}·2Br^-$-$13^{2+}·2Br^-$** (0.100g, 0.1 mmol) in CH$_2$Cl$_2$ (20 mL) was washed with a saturated solution of NH$_4$PF$_6$ in H$_2$O and stirred during 20 min (5 x 20 mL). The organic solvent was collected and dried with anhydrous Na$_2$SO$_4$. The solid was separated by filtration and the solvent was removed under reduced pressure, to give the PF$_6^-$ salt in quantitative yields.

Bis-imidazolium receptor $10^{2+}·2PF_6^-$. Yield 0.112 g (97%), ^1H NMR (600 MHz, CD$_3$CN/ CD$_3$OD (95/5 v/v)) δ 8.73 (2H, s), 8.15 (4H, d, J = 7.6 Hz), 8.03 (4H, d, J = 7.6 Hz), 7.65 (4H, t, J = 7.6 Hz), 7.58 (4H, t, J = 7.6 Hz), 7.25 (1H, t, J = 7.8 Hz), 6.76 (2H, dd, J = 1.8 Hz, J = 7.8 Hz), 6.66 (1H, s), 6.29 (4H, s), 5.09 (4H, s), 2.04 (12H, s), 1.85 (6H, s); ^{13}C NMR (100 MHz, CD$_3$CN) δ 144.4, 135.7, 132.2, 131.5, 131.3, 130.8, 130.7, 128.8, 128.0, 127.4, 126.5, 126.4, 125.2, 123.6, 123.6, 48.5, 45.5, 11.4, 9.9, 8.9 ppm; MS (ESI): m/z calc. for $[M^{2+}+PF_6^-]^+$ 849.35, found 849.35; mp = 167-169 ºC; Anal. Calcd for $C_{50}H_{48}F_{12}N_4P_2$: C, 60.36; H, 4.86; N, 5.63. Found: C, 60.20; H, 4.75; N, 5.60.

Bis-imidazolium receptor $11^{2+}·2PF_6^-$. Yield 0.112 g (98%), ^1H NMR (600 MHz, CD$_3$CN/ CD$_3$OD (95/5 v/v)) δ 8.74 (2H, s), 8.17 (4H, d, J = 8 Hz), 8.06 (4H, d, J = 8 Hz), 7.86 (2H, d, J = 8 Hz), 7.66 (4H, t, J = 6 Hz), 7.59 (4H, t, J = 6 Hz), 7.32 (2H, s), 7.08 (2H, dd, J = 8 Hz, J = 2 Hz), 6.33 (4H, s), 5.36 (4H, s), 2.15 (6H, s), 2.06 (6H, s), 2.02 (6H, s); ^{13}C NMR (100 MHz, CD$_3$CN) δ 144.4, 133.7, 133.3, 133.2, 132.2, 131.6, 131.3, 130.7, 129.8, 128.8, 128.0, 127.5, 126.4, 125.8, 125.2, 123.6, 49.0, 45.5, 11.6, 9.9, 9.0 ppm; MS (ESI): m/z calc. for $[M^{2+}+PF_6^-]^+$ 899.37, found 899.37; mp = 181-183 ºC; Anal. Calcd for $C_{54}H_{50}F_{12}N_4P_2$: C, 62.07; H, 4.82; N, 5.36. Found: C, 62.21; H, 4.87; N, 5.47.

Bis-imidazolium receptor 12²⁺·2PF₆⁻. Yield 0.111 g (96%), ¹H NMR (400 MHz, CD₃CN/ CD₃OD (95/5 v/v)) δ 8.74 (2H, s), 8.16 (4H, d, J = 8 Hz), 8.02 (4H, d, J = 8 Hz), 7.64 (4H, t, J = 6 Hz), 7.57 (4H, t, J = 6 Hz), 6.89 (4H, s), 6.30 (4H, s), 5.17 (4H, s), 2.07 (6H, s), 2.03 (6H, s), 1.93 (6H, s) ppm; ¹³C NMR (100 MHz, CD3CN) δ 144.3, 134.9, 132.2, 131.5, 131.2, 130.7, 128.8, 128.0, 127.6, 127.4, 126.4, 123.6, 48.5, 45.5, 11.5, 9.9, 8.9 ppm; MS (ESI): m/z calc. for [M²⁺+PF₆⁻]⁺ 849.35, found 849.35; mp = 167-169 ºC; Anal. Calcd for C₅₀H₄₈F₁₂N₄P₂: C, 60.36; H, 4.86; N, 5.63. Found: C, 60.42; H, 4.73; N, 5.69.

Bis-imidazolium receptor 13²⁺·2PF₆⁻. Yield 0.113 g (98%), ¹H NMR (600 MHz, CD₃CN/ CD₃OD (95/5 v/v)) δ 8.67 (2H, s), 8.11 (4H, d, J = 8 Hz), 7.94 (4H, d, J = 8 Hz), 7.78 (1H, t, J = 8 Hz), 7.59 (4H, t, J = 7 Hz), 7.53 (4H, t, J = 7 Hz), 7.21 (2H, d, J = 8 Hz), 6.15 (4H, s), 4.99 (4H, s), 1.87 (6H, s), 1.80 (6H, s), 1.72 (6H, s) ppm; ¹³C NMR (100 MHz, CD₃CN/ CD₃OD (95/5 v/v)) δ 154.0, 144.5, 139.8, 132.1, 131.5, 131.3, 130.7, 128.8, 127.4, 127.3, 126.4, 123.6, 123.4, 122.7, 49.9, 45.2, 11.2, 9.7, 8.7 ppm; MS (ESI): m/z calc. for [M²⁺+PF₆⁻]⁺ 850.3, found 850.3; mp = 158-160 ºC; Anal. Calcd for C₄₉H₄₇F₁₂N₅P₂: C, 59.10; H, 4.76; N, 7.03. Found: C, 59.25; H, 4.67; N, 6.93.

X-ray crystal structure analysis. Compound [13²⁺][PF₆]₂·(CH₃CN): weakly diffracting crystals were obtained by re-crystallization from CH₃CN/CH₃OH/ⁱPr₂O solution. C₅₁H₅₀F₁₂N₆P₂, M = 1036.91, monoclinic, a = 11.094(2), b = 13.316(3), c = 31.782(6) Å, $β$ = 94.03(3)º, U = 4683.1(16) Å³, space group P2(1)/n, Z = 4, T = 120(2) K, 34775 reflections measured, 13251 unique (R$_{int}$ = 0.0902). Methyl group hydrogen atoms refined as *rigid*, others *riding*. R1 (I > 2σ(I)) = 0.0674 and wR2 (all data) = 0.2260.[17]

ASSOCIATED CONTENT

Supporting Information Available: ¹H- and ¹³C-NMR spectra, Job plot experiments, ³¹P NMR, fluorescence and Uv-Vis anion binding studies, computational details and Cartesian coordinates and total energies of all species discussed in the text, Ellipsoid plot for **compound** [13²⁺][PF₆]₂·(CH₃CN), crystallographic information file (CIF) containing X-ray data of compound [13²⁺][PF₆]₂·(CH3CN). This material is available free of charge via the Internet at http://pubs.acs.org.

AUTHOR INFORMATION

Corresponding Authors

* Email: pmolina@um.es; antocaba@um.es.

ACKNOWLEDGMENT

REFERENCES

1 (a) Gale, P. A.; Busschaert, N.; Haynes, C. J. E.; Karagiannidis, L. E.; Kirby, I. L. *Chem. Soc. Rev.*, **2014**, *43*, 205-241; (b) Evans, N. H.; Beer, P. B., *Angew. Chem. Int. Ed.*, **2014**, *53*, 2-41. (c) Langton, M. J.; Serpell, C. J.; Beer, P. D. *Angew. Chem. Int. Ed.*, **2016**, 55, 1974-1987.

2 Cai, J.; Sessler, J. *Chem. Soc. Rev.*, **2014**, *43*, 6198-6213.

3 (a) Metrangolo, P.; Neukirch, H.; Pilati T.; Resnati, G. *Acc. Chem. Res.* **2005**, *38*, 386-395. (b) Erdélyi, M. *Chem. Soc. Rev.*, **2012**, *41*, 3547-3557. (c) Beale, T. M.; Chudzinski, M. G.; Sarwar, M. G.; Taylor, M. S. *Chem. Soc. Rev.*, **2013**, *42*, 1667-1680. (d) Gilday, L. C.; Robinson, S. W.; Barendt, T. A.; Langton, M. J.; Mullaney, B. R.; Beer, P. D. *Chem. Rev.*, **2015**, *115*, 7118-7195.

4 (a) Frontera, A.; Gámez, P.; Mascal, M.; Mooibroek, T. J.; Reeddijk, J. *Angew. Chem. Int. Ed.*, **2011**, *50*, 9564-9583. (b) Frontera, A. *Coord. Chem. Rev.*, **2013**, *257*, 1716-1727. (c) Fiol, J. J.; Barceló-Oliver,M.; Tasada, A.; Frontera, A.; Terrón A.; García-Raso, A. *Coord. Chem. Rev.*, **2013**, *257*, 2705-2715.

5 For review see: Molina, P.; Tárraga, A.; Otón, F. *Org. Biomol. Chem.*, **2012**, *10*, 1711-1724.

6 (a) Yoo, J.; Kim, S. K.; Sing, N. T.; Kim, K. S. *Chem. Soc. Rev.*, **2006**, *35*, 355-360. (b) Xu, Z.; Kim S. K.; Yoon, J. *Chem. Soc. Rev.*, **2010**, *39*, 1457-1466. (c) Marullo, S.; D´Anna, F. D.; Cascino, M.; Noto, R. *J. Org. Chem.*, **2013**, *78*, 10203-10208.

7 (a) Serpell, C. J.; Kilah, N. L.; Costa, P. J.; Felix, V.; Beer, P. D. *Angew. Chem. Int. Ed.*, **2010**, *49*, 5322-5326. (b) Caballero, A.; White, N. G.; Beer, P. D. *Angew. Chem., Int. Ed.* **2011**, *50*, 1845-1848. (c) Caballero, A.; Zapata, F.; White, N. G.; Costa, P. J.; Felix, V.; Beer, P. D. *Angew. Chem., Int. Ed.* **2012**, *51*, 1876-1880. (d) Cametti, M.; Raatikainen, K.; Metrangolo, P.; Pilati, T.; Terraneo, G.; Resnati, G. *Org. Biomol. Chem.*, **2012**, 1329-1333. (e) Zapata, F.; Caballero, A.; White, N. G.; W. Claridge, T. D.; Costa, P. J.; Felix V.; Beer, P. D. *J. Am. Chem. Soc.*, **2012**, *134*, 11533-11541;

8 Graeme, S. T.; Serpell, C. J.; Sardinha, J.; Costa, P. J.; Flix, V.; Beer, P. D. *Chem. Eur. J.* **2011**, *17*, 12955-12966.

9 (a) Farnham, W. B.; Roe, D. C.; Dixon, D. A.; Calabrese,J. C.; Harlo; Tocher, D. A.; Steed, J. W. *J. Am. Chem. Soc.*, **2004**, *126*, 12395-12402. (b) Zhu, S. S.; Staats, H.; Brandhorst, K.; Grunenberg, J.; Gruppi, F.; Dalcanale, E.; Luetzen, A.; Rissanen, K.; Schalley, C. A. *Angew. Chem. Int. Ed.* **2008**, *47*, 788-792. (c) Bedford, R. B.; Betham, M.; Butts, C. P.; Coles, S. J.; Hursthouse, M. B.; Scully, P. N.; Tucker, J. H.; Wilkie, J.; Willener, Y. *Chem. Commun.*, **2008**, 2429-2431. (d) Pandian, T. S.; Kang, J., *Tetrahedron Lett.*, **2015**, *56*, 4191-4194. (e) Senthil Pandian, T.; Srinivasadesikan, Venkatesan; Lin, M.C.; Kang, J. *Tetrahedron*, **2015**, *71*, 8350-8356.

10 Wolkenberg, S. E.; Wisnoski, D. D.; Leister, W. H.; Wang, Y.; Zhao, Z.; Lindsley, C. W. *Org. Lett.*, **2004**, *6*, 1453-1456.

11 (a) Mata, I.; Alkorta, I.; Molins, E.; Espinosa, E. *ChemPhysChem* **2012**, *13*, 1421-1424. (b) Mata, I.; Alkorta, I.; Molins, E.; Espinosa, E. *Chem. Phys. Lett.* **2013**, *555*, 106-109. (c) Zapata, F.; González, L.; Caballero, A.; Alkorta, I.; Elguero, J.; Molina, P. *Chem. Eur. J.* **2015**, *21*, 9797-9808.

12 Hynes, M. J. *J. Chem. Soc., Dalton Trans.* **1993**, 311-312.

13 (a) Ghosh, K.; Sarkar, A. R.; Samadder, A.; Khuda-Bukhsh, A. R. *Org. Lett.* **2012**, *14*, 4314-4317. b) Zapata, F.; Gonzalez, L.; Caballero, A.; Alkorta, I.; Elguero, J.; Molina, P. *Chem. Eur. J.* **2015**, *21*, 9797-9808.

14 (a) Yoon, J.; Kim, S. K.; Singh, N. J.; Lee, J. W.; Yang, Y. J.; Chellappan, K.; Kim, K. S. *J. Org. Chem.* **2004**, *69*, 581-583. (b) Kim, S. K.; N. Singh, J.; Kim, S. J.; Kim, H. G. J.; Kim, K. J.; Lee, W.; Kim, K. S.; Yoon, J. *Org. Lett.* **2003**, *5*, 2083-2086. (c) Kim, S. K.; Singh, N. J.; Kwon, J.; Hwang, I.-C.; Park, S. J.; Kimb, K. S.; Yoona, J. *Tetrahedron* **2006**, *62*, 6065-6072.

15 See computational details in the Supporting Information.

16 Bondi, A. *J. Phys. Chem. A*, **1964**, *68,* 441-451.

17　　CCDC-1456591　contains　the　supplementary　crystallographic　data　for　compound　**[13^{2+}][PF$_6$]$_2$·(CH$_3$CN)** (www.ccdc.cam.ac.uk/data_request/cif).

$A^- = HP_2O_7^{3-}$

$A^- = SO_4^{2-}$